

Contents

1

Table of Contents	2	2
List of Figures	3	3
List of Tables	4	4
1 Phylogeography	5	5
1.1 Introduction	5	6
1.2 Methods	8	7
1.2.1 Sampling and DNA Isolation	8	8
1.2.2 RADseq Library Preparation	9	9
1.2.3 Phylogenetic Data Processing	11	10
1.2.4 Maximum Likelihood	11	11
1.2.5 Multispecies Coalescent	12	12
1.2.6 Test for Historic Admixture	12	13
1.2.7 Population Structure Data Processing	13	14
1.2.8 Population Structure	13	15
1.2.9 Recent <i>A. fowleri</i> x <i>A. woodhousii</i> hybridization	14	16
1.3 Results	14	17
1.3.1 Assembly and alignment with <i>ipyrad</i>	14	18
1.3.2 Maximum Likelihood Phylogeny	15	19
1.3.3 Coalescent Phylogeny	15	20
1.3.4 Historic Introgression	16	21

1.3.5	Population Structure	17	22
1.3.6	Hybridization between <i>A. fowleri</i> and <i>A. woodhousii</i>	17	23
1.4	Discussion	17	24
1.4.1	Phylogenetic relationships	17	25
1.4.2	Divergence Time	18	26
1.4.3	Hybridization	20	27
1.4.4	Population Structure and Hybridization	21	28
1.4.5	Conclusion	22	29
	References	22	30
1.5	Figures	27	31
1.6	Tables	38	32

List of Figures

33

1.1.	Distribution of <i>americanus</i> group samples	28	34
1.2.	Iqtree	29	35
1.3.	Iqtree	30	36
1.4.	Multispecies coalescent phylogeny	31	37
1.5.	<i>f</i> -branch statistics	32	38
1.6.	Americanus Population Structure	33	39
1.7.	Fowleri Population Structure	34	40
1.8.	Terrestris Population Structure	35	41
1.9.	Woodhousii Population Structure	36	42
1.10.	Fowleri Population Structure	37	43

List of Tables

44

1.1 Samples used in this study	39	45
--	----	----

Chapter 1

46

Phylogeography

47

1.1 Introduction

48

Many factors are understood to be important in driving and shaping the diversification and evolutionary history of organisms. Chief among them is the interplay between climatic conditions and geologic processes. Changes in these environmental variables can alter the distributions of organisms and result in changes in the connectivity of populations. Disconnected populations may undergo genetic divergence from one another due to adaptive evolution in response to changing abiotic or biotic conditions. Or they might simply diverge via neutral evolution driven by the effects of drift. Environmental changes can also reconnect previously isolated populations resulting in hybridization and gene flow, another very important process shaping patterns of diversity. Understanding the interplay of all of these factors is critical for understanding the evolutionary history of organisms. A critical step to understanding these processes is to obtain an accurate reconstruction of the evolutionary history of organisms.

49

50

51

52

53

54

55

56

57

58

59

60

The North American toads in the genus *Anaxyrus* are a group of organisms with a poorly understood evolutionary history. Although, not for lack of trying. Multiple studies of the evolutionary relationships among species in the genus have produced conflicting results (Fontenot et al., 2011; Graybeal, 1997; Masta et al., 2002; Portik et al., 2023; Pramuk et al., 2007; Pyron & Wiens, 2011). Particularly within the *americanus* group

61

62

63

64

65

composed of *A. americanus*, *A. baxteri*, *A. fowleri*, *A. hemiophrys*, *A. houstonensis*,
66
A. microscaphus, *A. terrestris*, and *A. woodhousii*. Two phylogenetic studies inferred
67
trees with *A. fowleri* forming a polytomy making them inconsistent with the current
68
taxonomy of *Anaxyrus* (Fontenot et al., 2011; Masta et al., 2002). These conflicting
69
results could be due to methodological differences such as the species included, the number
70
of individuals of each species sequenced, inference methods used, or the sequenced loci.
71
But the differences in inferred relationships could also result from real biological processes.
72
Incomplete lineage sorting is one potential source of discordance among datasets which
73
include different loci that arises from real biological processes and impacts phylogenetic
74
inference (Kubatko & Degnan, 2007). Incomplete lineage sorting could also produce the
75
polytypic relationship among *A. fowleri*.
76

Gene flow is another potential source of discordance among genes which could drive
77
the differences in inferred relationships among studies using different loci and could also
78
produce the pattern seen in *A. fowleri* (Degnan & Rosenberg, 2009). While incomplete
79
lineage sorting is very likely to have impacted patterns of genetic variation in *Anaxyrus*,
80
gene flow due to hybridization is a distinct possibility as well. There are numerous
81
reports of natural hybridization between several different species of *Anaxyrus* (Green,
82
1996). A study of allozyme variation across a hybrid zone between *A. americanus* and
83
A. hemiophrys revealed introgression taking place across a more than 50km wide hybrid
84
zone. Hybrid zones are also suspected to exist between *A. americanus* and *A. terrestris*
85
and between *A. woodhousii* and *A. fowleri* though no study has yet been conducted to
86
characterize these putative hybrid zones (Green, 1996; Weatherby, 1982). Furthermore,
87
numerous laboratory crosses have been performed between pairs of *Anaxyrus* species with
88
currently overlapping distributions (Blair, 1963, 1972). Some of which produce viable and
89
fertile backcross progeny (Blair, 1963, 1972). These studies suggest that gene flow could
90
very easily have played a role in shaping patterns of diversity in *Anaxyrus*. However,
91
they provide only a snapshot in time with no indication of the long term consequences.
92
There are many potential consequences of hybridization such as adaptive introgression,
93
introgression of neutral genetic variation, reinforcement, lineage fusion, polyploidization,
94

hybrid speciation, or transition to unisexual reproduction (Abbott et al., 2013). Inference
95
of past introgression is an important starting point for exploring these outcomes yet it
96
remains a challenging problem. The network structure of phylogenetic networks are far
97
less tractable to infer than the more simple bifurcating phylogenies for which there has
98
been extensive method development. There has been some recent work to overcome this
99
challenge as well as increased feasibility of obtaining appropriate genome wide datasets
100
to investigate past gene flow.
101

Apart from the significant evolutionary implications of hybridization which need to
102
be understood, it also presents a valuable opportunity for investigating the mechanisms
103
that drive divergence and the evolution of reproductive incompatibility (Rieseberg et al.,
104
1999). Many generations of backcrossing within hybrid zones can produce a large number
105
of highly recombinant genomes that allow for the observation of many possible hybrid
106
genotypes under natural conditions in order to identify advantageous or disadvantageous
107
hybrid genotypes. In most species it is not feasible to produce such a large number of
108
highly recombinant offspring in order to make such observations. The evolutionary history
109
of hybridizing species is important context to have when studying patterns of introgression
110
within hybrid zones. Context such as the phylogenetic relationship of hybridizing
111
species relative to other closely related species, the amount of genetic differentiation, the
112
time since divergence and by extension the biogeographic processes driving initial diver-
113
gence and subsequent secondary contact in cases of allopatric divergence. This important
114
context is currently missing for *Anaxyrus* which limits the inferences that can be made
115
regarding hybrid zones in this genus.
116

Ultimately, environmental change is what leads many populations divergence and and
117
may lead to subsequent or concurrent gene flow. Therefore, environmental variables are
118
also important context for making inferences from hybrid zones in addition to under-
119
standing the process of diversification more generally. To date, there have not been any
120
studies conducted to understand how the environment as driven diversification in North
121
American toads. North America has had a very complex geologic and climatic history
122
(Lyman & Edwards, 2022). The effects of which are often clade specific (Nuñez et al.,
123

2023). But large scale environmental changes can impact multiple species simultaneously
124
(Oaks, 2019). There has been recent development in methods to infer these events (Oaks,
125
2019; Oaks et al., 2022). The identification of multiple pairs of lineages that underwent
126
divergence at the same time could provide evidence about environmental changes driving
127
diversification. Present day population structure could also provide further understanding
128
by revealing environmental factors that reduce gene flow assuming the biological limits
129
of present day species have not evolved dramatically from the ancestral condition.
130

In this study, I investigate the evolutionary history of North American toads in the
131
genus *Anaxyrus* using genome wide sequence data. For this I obtained restriction enzyme-
132
associated DNA sequence (RADseq) data from 12 species of *Anaxyrus* including dense
133
sampling representing a large portion of the ranges of *A. americanus*, *A. fowleri*, *A.*
134
terrestris, and *A. woodhousii*. With these data I infer evolutionary relationships using
135
maximum likelihood analysis of a concatenated dataset of many broadly distributed sam-
136
ples in addition to using a multispecies coalescent analysis of a subset of the data. I also
137
test for the presence of shared divergence times which might suggest *Anaxyrus* diversifi-
138
cation has been driven by the same environmental changes and also estimate the absolute
139
timing of all divergences within the genus. With the robust estimate of phylogenetic re-
140
lationships among *Anaxyrus* species, I test for the presence of past introgression among
141
species. In order to identify the types of environmental factors that might have played
142
a role in isolating populations that would eventually diverge as species, I investigate
143
population structure within a subset of *Anaxyrus* species. Finally, I estimate proportions
144
admixture between *A. fowleri* and *A. woodhousii* to test the hypothesis that these species
145
form a hybrid zone in the central United States where their ranges meet.
146

1.2 Methods 147

1.2.1 Sampling and DNA Isolation 148

I obtained tissue samples from museum tissue collections as well as from individuals I
149
collected from 2017 to 2020. I selected samples to represent as much of the range of each
150

species of *Anaxyrus* as possible. I also included one *Rhinella marina* and one *incilius nebulifer* for as outgroups for phylogenetic analyses. 151
152

I isolated DNA from tissues by first lysing a piece of tissue approximately the size 153
of a grain of rice in 300 μL of a solution of 10mM Tris-HCL, 10mM EDTA, 1% SDS 154
(w/v), and nuclease free water along with 6 mg Proteinase K that was incubated for 4-16 155
hours at 55°C in a 1.5 mL microcentrifuge tube. To purify the DNA and separate it from 156
the lysis product, I mixed the lysis product with a 2X volume of SPRI bead solution 157
containing 1 mM EDTA, 10 mM Tris-HCl, 1 M NaCl, 0.275% Tween-20 (v/v), 18% PEG 158
8000 (w/v), 2% Sera-Mag SpeedBeads (GE Healthcare PN 65152105050250) (v/v), and 159
nuclease free water. I then incubated the samples at room temperature for 5 minutes, 160
placed the beads on a magnetic rack, and discarded the supernatant once the beads had 161
collected on the side of the tube. I then performed two ethanol washes by adding 1 mL of 162
70% ETOH to the beads while still placed in the magnet stand and allowing it to stand 163
for 5 minutes before discarding the ethanol. After removing all ethanol from the second 164
wash, I removed the tube from the magnet stand and allowed the sample to dry for 1 165
minute before mixing the beads with 100 μL of TLE solution containing 10 mM Tris- 166
HCL, 0.1 mm EDTA, and nuclease free water. After allowing the bead mixture to stand 167
at room temperature for 5 minutes I returned the beads to the magnet stand, pipetted 168
all of the TLE solution into another microcentrifuge tube, and discarded the beads. I 169
quantified DNA with a Qubit fluorometer (Life Technologies, USA) and diluted samples 170
with TLE solution to bring the concentration to 20 ng/ μL . 171

1.2.2 RADseq Library Preparation 172

I prepared RADseq libraries using the 2RAD approach outlined by Bayona-Vásquez 173
et al., 2019. On 96 well plates, I ligated 100 ng of sample DNA in 15 μL of a solution 174
with 1X CutSmart Buffer (New England Biolabs, USA; NEB), 10 units of XbaI, 10 units 175
of EcoRI, 0.33 μM XbaI compatible adapter, 0.33 μM EcoRI compatible adapter, and 176
nuclease free water with a 1 hour incubation at 37°C. I then immediately added 5 μL of 177
a solution with 1X Ligase Buffer (NEB), 0.75 mM ATP (NEB), 100 units DNA Ligase 178

(NEB), and nuclease free water and incubated at 22°C for 20 min and 37°C for 10 min for
179 two cycles, followed by 80°C for 20 min to stop enzyme activity. For each 96 well plate,
180 I pooled 10 μ L of each sample and split this pool equally between two microcentrifuge
181 tubes. I purified each pool of libraries with a 1X volume of SpeedBead solution followed
182 by two ethanol washes as described in the previous section except that the DNA was
183 resuspended in 25 μ L of TLE solution.
184

In order to be able to detect and remove PCR duplicates, I performed a single cycle
185 of PCR with the iTru5-8N primer which adds a random 8 nucleotide barcode to each
186 library construct. For each plate, I prepared four PCR reactions with a total volume of
187 50 μ L containing 1X Kapa Hifi Buffer (Kapa Biosystems, USA; Kapa), 0.3 μ M iTru5-8N
188 Primer, 0.3 mM dNTP, 1 unit Kapa HiFi DNA Polymerase, 10 μ L of purified ligation
189 product, and nuclease free water. I ran reactions through a single cycle of PCR on a
190 thermocycler at 98°C for 2 min, 60°C for 30 s, and 72°C for 5 min. I pooled all of the
191 PCR products for a plate into a single tube and purified the libraries with a 2X volume
192 of SpeedBead solution as described before and resuspended in 25 μ L TLE. I added the
193 remaining adapter and index sequences unique to each plate with four PCR reactions with
194 a total volume of 50 μ L containing 1X Kapa Hifi (Kapa), 0.3 μ M iTru7 Primer, 0.3 μ M
195 P5 Primer, 0.3 mM dNTP, 1 unit of Kapa Hifi DNA Polymerase (Kapa), 10 μ L purified
196 iTru5-8N PCR product, and nuclease free water. I ran reactions on a thermocycler with
197 an initial denaturation at 98°C for 2 min, followed by 6 cycles of 98°C for 20 s, 60°C
198 for 15 s, 72°C for 30 s and a final extension of 72°C for 5 min. I pooled all of the PCR
199 products for a plate into a single tube and purified the product with a 2X volume of
200 SpeedBead solution as described before and resuspended in 45 μ L TLE.
201

I size selected the library DNA from each plate in the range of 450-650 base pairs using
202 a BluePippin (Sage Science, USA) with a 1.5% dye free gel with internal R2 standards.
203 To increase the final DNA concentrations I prepared four PCR reactions for each plate
204 with 1X Kapa Hifi (Kapa), 0.3 μ M P5 Primer, 0.3 μ M P7 Primer, 0.3 mM dNTP, 1 unit
205 of Kapa HiFi DNA Polymerase (Kapa), 10 μ L size selected DNA, and nuclease free water
206 and used the same thermocycling conditions as the previous (P5-iTru7) amplification. I
207

pooled all of the PCR products for a plate into a single tube and purified the product with
208 a 2X volume of SpeedBead solution as before and resuspended in 20 μ L TLE. I quantified
209 the DNA concentration for each plate with a Qubit fluorometer (Life Technologies, USA)
210 then pooled each plate in equimolar amounts relative to the number of samples on the
211 plate and diluted the pooled DNA to 5 nM with TLE solution. The pooled libraries were
212 pooled with other projects and sequenced on an Illumina HiSeqX by Novogene (China)
213 to obtain paired end, 150 base pair sequences.
214

1.2.3 Phylogenetic Data Processing

215

To produce alignments for phylogenetic analysis, I first I demultiplexed the iTru7
216 indexes using the *process_radtags* command from *Stacks* v2.6.4 (Rochette et al., 2019)
217 and allowed for two mismatches for rescuing reads. I removed PCR duplicates using the
218 the *clone_filter* command from *Stacks*. To demultiplex individual samples I used *ipyRAD*
219 v0.9.90 and allowed for one mismatch for rescuing reads. I assembled and aligned reads
220 with *ipyRAD* using default parameters and a clustering threshold of 0.8. Using *ipyRAD*, I
221 filtered loci not present in at least 75% of samples and filtered samples with fewer than
222 200 loci.
223

1.2.4 Maximum Likelihood

224

Phylogenetic methods that do not account for incomplete lineage sorting do not per-
225 form well with data impacted by this process. However, methods that do account for
226 incomplete lineage sorting are far more computationally demanding. As a result, these
227 methods cannot be performed with a large number of samples. I therefore conducted con-
228 ducted maximum likelihood phylogenetic inference in order to infer a phylogeny with all
229 of the sequenced samples and to be able to identify samples that may be problematic for
230 other methods due to recent admixture or data quality. I conducted the maximum likeli-
231 hood phylogenetic inference with *IQ-TREE* v1.6.12 (Nguyen et al., 2015) with the *ipyRAD*
232 alignment as input in order. I ran *IQ-TREE* with 1000 ultrafast bootstrap replicates
233 (Hoang et al., 2018) under the GTR substitution model.
234

1.2.5 Multispecies Coalescent 235

In order to account for incomplete lineage sorting in the inference of phylogenetic 236 relationships and to infer shared divergence times, I used the program *phycoeval*. I 237 selected a subset of up to four samples from each species due to the infeasible run times 238 for *phycoeval* with greater numbers of samples (see table 1). I excluded sample 006 from 239 consideration due it having an anomalous position in the maximum likelihood tree. I 240 used *ipyrad* to filter loci not present in at least 75% of samples. Using a custom script I 241 filtered the phylip alignment file produced by *ipyrad* to exclude sites with more than two 242 characters and output the filtered alignment to nexus format with a biallelic character 243 encoding. I ran *phycoeval* with state frequencies fixed at 0.5. I set the mutation rate 244 equal to one so that divergence times are in units of expected substitutions per site. I 245 set the prior on the age of the root as an exponential distribution with a mean of 0.01. 246 I ran *phycoeval* with the assumption of a single effective population size shared across 247 all of the branches of the tree. The prior on the effective population size was a gamma 248 prior with a shape of four and mean of 0.0005 I ran five independent MCMC chains 249 for 10,000 generations, sampling every 10 generations. Each chain was started with a 250 comb tree topology with all branches sharing the same divergence time. I summarized 251 the posterior sample of tree topologies and parameters using *sumphycoeval*. To assess 252 convergence and mixing, I used *sumphycoeval* to calculate the potential scale reduction 253 factor (PSRF) and the effective sample size (ESS). I discarded the first 100 samples from 254 each chain as burnin. I used *sumphycoeval* to rescale the branch lengths of the maximum 255 a posteriori (MAP) tree produced by *sumphycoeval* so that the posterior mean root age 256 was 16.5 million years ago based on the estimate of Feng et al., 2017. 257

1.2.6 Test for Historic Admixture 258

In order to test for a history of introgression between species of *Anaxyrus* I used the 259 program *dsuite* v0.5r50 (Malinsky et al., 2021) to compute the *f*-branch statistic for each 260 pair of *Anaxyrus* species for which the statistic can be calculated (Malinsky et al., 2018; 261 Reich et al., 2009). I used *ipyrad* to filter all loci that were not found in at least 50% of 262

the samples that passed filtering and excluded one *A. fowleri* sample (sample 006 from ??) which falls outside of the *A. fowleri* clade inferred by *IQ-TREE*. For the input tree topology required to run *dsuite*, I used the topology inferred by *phycoeval* and I specified *Incilius nebulifer* as the outgroup species. I ran the *dsuite* Dtrios command to compute Patterson's the *f*4-ratio statistic for all possible trios with 20 block-jackknife replicates. I then ran the Fbranch command from *dsuite* to compute the *f*-branch statistics from the computed *f*4-ratio statistics. I plotted the *f*-branch statistics with *dtools* v0.1 which is packaged with the *dsuite* program (Malinsky et al., 2021).

Say something about how *f*-branch takes into account correlation among branches 271

1.2.7 Population Structure Data Processing 272

I processed reads differently for the analysis of population structure following PCR duplicate filtering. I demultiplexed individual samples, trimmed adapter sequence, and filtered reads with low quality scores as well as reads with any uncalled bases using the *process_radtags* command and allowed for the rescue of restriction site sequence as well as barcodes with up to two mismatches. I allowed for 14 mismatches between alleles within, as well as between individuals (M and n parameters). This is equivalent to a sequence similarity threshold of 90% for the 140 bp length of reads post trimming. I also allowed for up to 7 gaps between alleles within and between individuals. I used the *populations* command from *Stacks* to filter loci missing in more than 5% of individuals, filter all sites with minor allele counts less than 3, filter any individuals with more than 90% missing loci, and randomly sample a single SNP from each locus.

1.2.8 Population Structure 284

To investigate population structure within *A. americanus*, *A. fowleri*, *A. terrestris*, and *A. woodhousii*, I used the demultiplexed and de-cloned reads used for the phylogenetic analyses for producing alignments. I assembled and aligned these reads using *Stacks* for each species separately. I allowed for 7 mismatches between alleles within, as well as between individuals (M and n parameters). This is equivalent to a sequence similarity

threshold of 95% for the 140 bp length of reads post trimming. I also allowed for up to
290
7 gaps between alleles within and between individuals. I used the *populations* command
291
from *Stacks* to filter loci missing from more than 5% of samples, filter all sites with minor
292
allele counts less than 3, filter any individuals with more than 90% missing loci and to
293
randomly sample a single site per locus.
294

I ran the program *STRUCTURE* v2.3.4 (Pritchard et al., 2000) for each species
295
separately using the admixture model in order to cluster individuals and estimate ancestry
296
proportions for each individual. I ran *STRUCTURE* under four different models differing
297
in the number of populations assumed (K parameter), with the parameter ranging from 1-
298
4. I ran 10 iterations of *STRUCTURE* for each value of K for a total of 100,000 steps and
299
burnin of 50,000 for each iteration. I used the R package *POPHELP* v2.3.1 (Francis,
300
2017) to combine iterations for each value of K and to select the model producing the
301
largest ΔK which is the the model that has the greatest increase in likelihood score
302
from the previous model having one fewer populations as described by (Evanno et al.,
303
2005). I also investigated population structure with a non-parametric approach, using
304
principle component analysis (PCA) implemented in the R package *adegenet* *adegenet*
305
v2.1.10 (Jombart, 2008).
306

1.2.9 Recent *A. fowleri* x *A. woodhousii* hybridization

307

1.3 Results

308

1.3.1 Assembly and alignment with *ipyrad*

309

A total of 436,265,266 reads were obtained for all samples. After filtering low quality
310
reads and reads without restriction site sequence, 435,650,926 total reads remained for
311
assembly. The number of filtered reads per individual was highly variable with a mean of
312
4,538,030 ($sd=3,619,076$). Prior to filtering there were 171,174 loci total loci which was
313
reduced to 659 after filtering loci not present in at least 75% of samples and filtering ??
314
samples which had fewer than 200 loci (Table 1). Mean sequence read coverage of the
315

loci passing filter was 54x. The final alignment contained a total of 184,453 sites with
316
20,361 SNPs with 14.96% of sites and 14.71% of SNPs missing.
317

1.3.2 Maximum Likelihood Phylogeny

318

The full majority rule consensus tree inferred by *IQ-TREE* is presented in 1.2. All
319
species were inferred as a single monophyletic group with the exception of *A. fowleri*. A
320
A. fowleri sample (sample 006) does not form a monophyletic group with other
321
A. fowleri samples but is instead sister to the branch containing *A. woodhousii* and
322
A. fowleri samples. A representation of the tree inferred by *IQ-TREE* with the tips
323
within species specific clades collapsed is presented in 1.3. Each species specific clade for
324
which there are at least two representatives samples all have ultrafast bootstrap support
325
values of 100%. All branches below the level of the species specific clades have
326
ultrafast bootstrap support values ranging from 70-100% with the majority being 100%.
327
The most basal internal branch of the tree, marking the split between most of *Anaxyrus*
328
and *A. punctatus* along with the outgroup *Incilius nebulifer* has an ultrafast bootstrap
329
support value of 99%. The sister branch to *A. terrestris*, which contains the spurious
330
A. fowleri sample (sample 006) and the clade containing *A. fowleri* and *A. woodhousii*,
331
has an ultrafast bootstrap support value of 96%. The lowest ultrafast bootstrap support
332
value is found on the branch sister to the *A. cognatus/A. speciosus* clade with a value of
333
only 70%.
334

1.3.3 Coalescent Phylogeny

335

The maximum a posteriori (MAP) tree inferred under the multispecies coalescent
336
model using *phycoeval* has a topology differs from the maximum likelihood topology
337
inferred by *IQ-TREE* Fig. 1.4. The MAP tree produced by *phycoeval* does not have any
338
shared divergence times among any of the 10 internal nodes of the tree. The frequency
339
of topologies in the posterior sample that have 10 independent divergence times is 0.5.
340
The next most frequent topology in the posterior are topologies with a single shared
341
divergence time and nine independent divergences and occur with a frequency of 0.24.
342

One major difference between the maximum likelihood tree inferred by *IQ-TREE* and 343
the MAP tree inferred by *phycoeval* is that the MAP tree has one multifurcation. This 344
multifurcation happens at the ancestor of the *A. quercicus*, *A. speciosus*/*A. cognatus*, 345
and *A. americanus* group lineages. However, this node has a low posterior probability of 346
only 0.51. All other branches in the MAP tree have high posterior probabilities of 0.98 347
or more. Most divergence events within *Anaxyrus* have occurred in the past 3.5 million 348
years and most diversification within the *A. americanus* group is less than 2.5 million 349
years old. 350

1.3.4 Historic Introgression 351

I used the program *dsuite* to compute the *f*-branchstatistic which is an estimate 352
of excess allele sharing between species pairs that is not due to incomplete lineage 353
sorting. I used the species tree topology produced by *phycoeval* for estimating the 354
f-branchstatistics. The *f*-branchestimates for each species pair are presented with a 355
heatmap in figure 1.5. Most *f*-branchestimates produced by *dsuite* were zero or very 356
near zero. Only 24 out of 112 *f*-branchestimates were greater than 0 and 11 of those 357
were greater than 0.05 Fig. 1.5. *A. americanus* and *A. woodhousii* had the largest number 358
of estimates greater than zero associated with them with nearly every pairwise comparison 359
greater than 0 Fig. 1.5. The highest *f*-branchstatistic values are between *A. americanus* 360
and two other species: *A. hemiophrys* (0.24) and *A. baxteri* (0.22) Fig. 1.5. The values 361
associated with *A. woodhousii* are appreciably lower with none exceeding 0.1 ???. The 362
branch preceding *A. speciosus* and *A. cognatus* tested against *A. punctatus* along with 363
the tests of *A. quercicus* with *A. cognatus* and *A. speciosus* all exceeded 0.1. 364

1.3.5 Population Structure	365
----------------------------	-----

1.3.6 Hybridization between <i>A. fowleri</i> and <i>A. woodhousii</i>	366
--	-----

1.4 Discussion	367
----------------	-----

1.4.1 Phylogenetic relationships	368
----------------------------------	-----

The maximum likelihood tree inferred by *IQ-TREE* Fig. 1.2 and ?? differs from trees inferred in previous studies of the relationships among *Anaxyrus* (Fontenot et al., 2011; Graybeal, 1997; Masta et al., 2002; Portik et al., 2023; Pramuk et al., 2007; Pyron & Wiens, 2011). Even among these previous studies there has been a great deal of inconsistency in the inferred relationships with the exception of a few taxa. As in all previous studies, the maximum likelihood tree inferred in this study places *A. punctatus* sister to all other *Anaxyrus*. I also found the *americanus* group to be monophyletic with *A. microscaphus* sister to all other *americanus* group species which is consistent with most previous studies. Two previous studies have inferred trees which do not place *A. fowleri* samples into a single monophyletic group (Fontenot et al., 2011; Masta et al., 2002). A single *A. fowleri* sample included in this study does not fall within a monophyletic group with the remaining *A. fowleri* samples but is instead sister to the clade containing all *A. fowleri* and *A. woodhousii* samples Fig. 1.3.

All of these studies have included different species, individuals, and loci, and also used different methods for alignment and phylogenetic inference. These differences in study design could result in the observed topology differences. The choice of locus in particular has a high likelihood of being the cause of these difference. Due to incomplete lineage sorting, the true histories of each gene may in fact differ (Kingman, 1982). The practice of concatenating multiple loci as all of the previous studies of *Anaxyrus* evolutionary relationships have done, can produce erroneous trees with high statistical support (Kubatko & Degnan, 2007).

To account for incomplete lineage sorting, I also inferred phylogenetic relationships among *Anaxyrus* species using the multispecies coalescent method *phycoeval* along with

a subset of individuals used for the maximum likelihood tree due to increased computational demands of multispecies coalescent methods. The topology of the *phycoeval* tree is substantially different from the maximum likelihood tree inferred in this study as well as trees from previous studies Fig. 1.4 (Fontenot et al., 2011; Graybeal, 1997; Masta et al., 2002; Portik et al., 2023; Pramuk et al., 2007; Pyron & Wiens, 2011). Unlike in any previous study or in the maximum likelihood tree, *A. americanus* and *A. terrestris* are placed sister to one another, whereas in all other trees it has had closer affinity to the *A. hemiophrys/A. baxteri* clade Fig. 1.3 (Portik et al., 2023; Pyron & Wiens, 2011). In the *phycoeval* tree, the *A. hemiophrys/A. baxteri* clade is instead sister to the *A. americanus/A. fowleri/A. terrestris/A. woodhousii* clade.

An unusual feature of *phycoeval* is that it can allow for multifurcations in inferred topologies (Oaks et al., 2022). This feature proved relevant for in this study as the inferred tree included one multifurcation at the ancestral node of *A. quercicus*, the *A. cognatus/A. speciosus* clade, and the *americanus* group.

Previous studies have produced trees with quite short internode branches at this part of the tree as did the *IQ-TREE* analysis in this study which is somewhat consistent with this. These methods can only produce bifurcations and thus would force any true multifurcation into bifurcations and estimate some branch length between them which would be expected to be short. In the *phycoeval* tree, the posterior probability of this split is low (0.51) so it may not be a perfect representation of the history of these lineages Fig. 1.4. More data may be necessary to have full resolution in this part of the tree. But it is clear that these three lineages diverged at least in rapid succession if not simultaneously. But I don't know of any significant implications these alternative scenarios would have for our understanding of *Anaxyrus* evolution.

1.4.2 Divergence Time

Only three previous studies have produced estimates for age of the *Anaxyrus* lineage ??????. The ?? phylogeny places *Incilius* sister to *Rhinella* rather than *Incilius* which is not supported by most recent studies making the approximately 23 mya estimate for the

origin of the genus questionable ??????. ?? estimate the split between *Anaxyrus* and *Incilius* to be 20.3 mya (95% HPD: 17.8-22.5) whereas ?? estimate a much earlier age of 16.5 mya (95% CI: 14.0-19.4). The dataset from ?? included near complete coverage from 95 nuclear loci whereas the ?? has a higher degree of missing data (95%) and includes both mitochondrial as well as nuclear loci. For these reasons I consider the ?? estimate to be the most reliable and chose it for the rescaling the branch lengths of the *phycoeval* tree. 420
421
422
423
424
425
426

Scaling the root of the *phycoeval* tree I estimated with the ?? estiate puts the time since the most recent common ancestor (MRCA) of extant *Anaxyrus* some time between 11.9 mya when *A. punctatus* diverged from other *Anaxyrus* and 16.5 mya when *Anaxyrus* split form *Incilius* 1.4. This range is is not inconsistent with the estimate of 12.3 mya (95% CI: 9.7-15.2) made by ?. But it would suggests that it must have happened almost immediately before the split leading to *A. punctatus*. ?? estimate the age of MRCA of *Anaxyrus* to be approximately halfway between the 14.7 mya *A. punctatus* split and the 20.3 mya split with *Incilius* at 16.7 mya. This study and the previous ones, have a high degree of uncertainty around the ages of these basal splits in the *Anaxyrus* tree. But it seems that that the split between *Incilius* and *Anaxyrus* likely happened somewhere around the start or just before the middle of the Miocene epoch. The MRCA of *Anaxyrus* and the split between the *boreas* group with a Western distribution, likely occurred prior to the middle of the Miocene. My estimate for the split between *A. punctatus* and other *Anaxyrus* would be right at the middle of the Miocene at a time when both precipitation and temperature underwent a decline in the North American interior and there was expansion of grasslands ?. The timing of the multifurcation of the *A. quercicus*, *A. cognatus/A. speciosus*, and *americanus* group lineages coincides with a previously identified shift in the ecomorphology of ungulate mammals inhabiting North America ?. 427
428
429
430
431
432
433
434
435
436
437
438
439
440
441
442
443
444
445

I estimate that diversification of the *americanus* group has all happened in the past 3.4 million years. This accounts for a large portion of the diversity of *Anaxyrus* and includes two additional un-sampled species which other studies have found to be nested within 446
447
448

this clades ?????. Those being *A. houstonensis* and *A. californicus*. This means that 449
most diversification within *Anaxyrus* took place just before and during the Pleistocene. 450
This was a period marked by a period of extreme climatic variation and repeated glacial 451
cycles that transformed the climate and geography of the North American continent 452
Surprisingly, there is no evidence from the *phycoeval* analysis that any of these cycles was 453
a driver of multiple diversification events and instead each of them occurred independently 454
during this period of *Anaxyrus* evolution. 455

1.4.3 Hybridization 456

Move all discussion of hybridization here. Given the interest of hybridization in 457
Anaxyrus and the promise of this group for understanding speciation it is important 458
to consider the implications of these relationships with regards to hybridization. 459

A. americanus and *A. terrestris* are sister *A. fowleri* and *A. woodhousii* are sister This 460
makes more sense with regards to hybridization between these two pairs of species and 461
better explains the sympatry of *A. americanus* and *A. terrestris* with *A. fowleri* and *A. 462
woodhousii*. This does make the hybrid zone between *A. americanus* and *A. hemiophrys* 463
more surprising. This hybrid zone is quite narrow however. 464

Considering the relationships of the maximum likelihood tree with respect to hy- 465
bridization, it is unsurprising to see *A. fowleri* (excluding sample 006) and *A. woodhousii* 466
to be each other's closest relatives and separated by relatively short branch lengths. 467

Not clear if *A. fowleri* sample placement is due to incomplete lineage sorting or due to 468
admixture. It does not fit the pattern of previous studies and is located near the contact 469
zone of *A. woodhousii* and *A. fowleri*. Furthermore the *STRUCTURE* analysis suggests 470
this sample has a lot of admixture which I discuss later. 471

A. americanus and *A. terrestris* on the other hand is more surprising. *A. terrestris* is 472
more closely related to *A. fowleri* than *A. americanus*, yet their ranges completely overlap 473
and they appear to have strong reproductive isolation. *A. americanus* has a range that 474
overlaps significantly with both *A. woodhousii* and *A. fowleri* but also appears to have 475
strong reproductive isolation with it's sympatric congeners. 476

The relationship between *A. hemiophrys* and *A. americanus* 477
A. hemiophrys and *A. americanus* are separated but much longer branch lengths on 478
the other but do not share any close relatives with which they. But The relationship 479
between *A. americanus* and *A. hemiophrys* is also unsurprising. Despite not being each 480
others The *A. americanus* and *A. hemiophrys* as well as *A. americanus* and *A. terrestris* 481
pairs do not 482

If we consider these relationships with regards to hybrid zones Interestingly, only a 483
single species pair (*A. fowleri* and *A. woodhousii*) for which there is evidence of a hybrid 484
zone are each other's closest relatives. The branch lengths between *A. americanus* and 485
A. hemiophrys as well as between *A. americanus* and *A. terrestris* are long relative to 486
the branches separating *A. woodhousii* and *A. fowleri*. 487

A. terrestris and *A. fowleri* are 488

Notably, only one species pair (*A. fowleri* and *A. woodhousii*) for which there is 489
evidence a hybrid zone are sister to each other. *A. americanus* and *A. hemiophrys* are 490
close to sister as *A. hemiophrys* and *A. baxteri* have little genetic difference between them 491
Fig. 1.2. It is interesting that *A. americanus* and *A. terrestris* form a hybrid zone while 492
A. fowleri and *A. terrestris* which are more closely related in sympatry. 493

1.4.4 Population Structure and Hybridization 494

Given the appearance that there are many secondary contact zones. It seems probable 495
that toad species have undergone range expansions. Following these range expansions, 496
are there any barriers that are now reducing gene flow? We can test that by looking 497
for population structure within species that aligns with possible biogeographic barriers. 498
The maximum likelihood tree along with the *STRUCTURE* analyses do not support the 499
existence of any unrecognized species diversity or significant population structure as some 500
mitochondrial studies have suggested. 501

Population structure in *A. woodhousii* with two overlapping mtDNA clades with 502
one more associated with the Southwest and one more associated with the great planes 503
(Masta et al., 2003) 504

1.4.5 Conclusion	505
References	506
Abbott, R., Albach, D., Ansell, S., Arntzen, J. W., Baird, S. J. E., Bierne, N., Boughman, J., Brelandsford, A., Buerkle, C. A., Buggs, R., Butlin, R. K., Dieckmann, U., Eroukhmanoff, F., Grill, A., Cahan, S. H., Hermansen, J. S., Hewitt, G., Hudson, A. G., Jiggins, C., ... Zinner, D. (2013). Hybridization and speciation. <i>Journal of Evolutionary Biology</i> , 26(2), 229–246. https://doi.org/10.1111/j.1420-9101.2012.02599.x	507
Bayona-Vásquez, N. J., Glenn, T. C., Kieran, T. J., Pierson, T. W., Hoffberg, S. L., Scott, P. A., Bentley, K. E., Finger, J. W., Louha, S., Troendle, N., Diaz-Jaimes, P., Mauricio, R., & Faircloth, B. C. (2019). Adapterama III: Quadruple-indexed, double/triple-enzyme RADseq libraries (2RAD/3RAD). <i>PeerJ</i> , 7, e7724. https://doi.org/10.7717/peerj.7724	513
Blair, W. F. (1963). Intragroup genetic compatibility in the <i>Bufo americanus</i> species group of toads. <i>The Texas Journal of Science</i> , 13, 15–34.	518
Blair, W. F. (1972). <i>Evolution in the genus Bufo</i> . University of Texas Press.	519
Degnan, J. H., & Rosenberg, N. A. (2009). Gene tree discordance, phylogenetic inference and the multispecies coalescent. <i>Trends in Ecology & Evolution</i> , 24(6), 332–340. https://doi.org/10.1016/j.tree.2009.01.009	521
Evanno, G., Regnaut, S., & Goudet, J. (2005). Detecting the number of clusters of individuals using the software structure: A simulation study. <i>Molecular Ecology</i> , 14(8), 2611–2620. https://doi.org/10.1111/j.1365-294X.2005.02553.x	524
Feng, Y.-J., Blackburn, D. C., Liang, D., Hillis, D. M., Wake, D. B., Cannatella, D. C., & Zhang, P. (2017). Phylogenomics reveals rapid, simultaneous diversification of three major clades of Gondwanan frogs at the Cretaceous–Paleogene boundary. <i>Proceedings of the National Academy of Sciences</i> , 114(29). https://doi.org/10.1073/pnas.1704632114	527

Fontenot, B. E., Makowsky, R., & Chippindale, P. T. (2011). Nuclear–mitochondrial	532
discordance and gene flow in a recent radiation of toads. <i>Molecular Phylogenetics</i>	533
and <i>Evolution</i> , 59(1), 66–80. https://doi.org/10.1016/j.ympev.2010.12.018	534
Francis, R. M. (2017). POPHELPER: An R package and web app to analyse and visualize	535
population structure. <i>Molecular Ecology Resources</i> , 17(1), 27–32. https://doi.org/10.1111/1755-0998.12509	536
Graybeal, A. (1997). Phylogenetic relationships of bufonid frogs and tests of alternate	538
macroevolutionary hypotheses characterizing their radiation. <i>Zoological Journal</i>	539
of the Linnean Society, 119(3), 297–338. https://doi.org/10.1111/j.1096-3642.1997.tb00139.x	540
Green, D. M. (1996). The bounds of species: Hybridization in the <i>Bufo americanus</i> group	542
of North American toads. <i>Israel Journal of Zoology</i> , 42, 95–109.	543
Hoang, D. T., Chernomor, O., von Haeseler, A., Minh, B. Q., & Vinh, L. S. (2018).	544
UFBoot2: Improving the Ultrafast Bootstrap Approximation. <i>Molecular Biology</i>	545
and <i>Evolution</i> , 35(2), 518–522. https://doi.org/10.1093/molbev/msx281	546
Huerta-Cepas, J., Serra, F., & Bork, P. (2016). ETE 3: Reconstruction, Analysis, and Vi-	547
ualization of Phylogenomic Data. <i>Molecular Biology and Evolution</i> , 33(6), 1635–	548
1638. https://doi.org/10.1093/molbev/msw046	549
Jombart, T. (2008). Adegenet : A R package for the multivariate analysis of genetic mark-	550
ers. <i>Bioinformatics</i> , 24(11), 1403–1405. https://doi.org/10.1093/bioinformatics/btn129	551
Kingman, J. (1982). The coalescent. <i>Stochastic Processes and their Applications</i> , 13(3),	553
235–248. https://doi.org/10.1016/0304-4149(82)90011-4	554
Kubatko, L. S., & Degnan, J. H. (2007). Inconsistency of Phylogenetic Estimates from	555
Concatenated Data under Coalescence (T. Collins, Ed.). <i>Systematic Biology</i> , 56(1),	556
17–24. https://doi.org/10.1080/10635150601146041	557
Lyman, R. A., & Edwards, C. E. (2022). Revisiting the comparative phylogeography of	558
unglaciated eastern North America: 15 years of patterns and progress. <i>Ecology and</i>	559
<i>Evolution</i> , 12(4), e8827. https://doi.org/10.1002/ece3.8827	560

- Malinsky, M., Matschiner, M., & Svardal, H. (2021). Dsuite - Fast D-statistics and related admixture evidence from VCF files. *Molecular Ecology Resources*, 21(2), 584–595. 561
<https://doi.org/10.1111/1755-0998.13265> 562
 563
- Malinsky, M., Svardal, H., Tyers, A. M., Miska, E. A., Genner, M. J., Turner, G. F., & Durbin, R. (2018). Whole-genome sequences of Malawi cichlids reveal multiple radiations interconnected by gene flow. *Nature Ecology & Evolution*, 2(12), 1940–1955. 564
<https://doi.org/10.1038/s41559-018-0717-x> 565
 566
 567
- Masta, S. E., Laurent, N. M., & Routman, E. J. (2003). Population genetic structure of the toad *Bufo woodhousii* : An empirical assessment of the effects of haplotype extinction on nested cladistic analysis. *Molecular Ecology*, 12(6), 1541–1554. https://doi.org/10.1046/j.1365-294X.2003.01829.x 568
 569
 570
 571
- Masta, S. E., Sullivan, B. K., Lamb, T., & Routman, E. J. (2002). Molecular systematics, hybridization, and phylogeography of the *Bufo americanus* complex in Eastern North America. *Molecular Phylogenetics and Evolution*, 24(2), 302–314. https://doi.org/10.1016/S1055-7903(02)00216-6 572
 573
 574
 575
- Nguyen, L.-T., Schmidt, H. A., von Haeseler, A., & Minh, B. Q. (2015). IQ-TREE: A Fast and Effective Stochastic Algorithm for Estimating Maximum-Likelihood Phylogenies. *Molecular Biology and Evolution*, 32(1), 268–274. https://doi.org/10.1093/molbev/msu300 576
 577
 578
 579
- Nuñez, L. P., Gray, L. N., Weisrock, D. W., & Burbrink, F. T. (2023). The phylogenomic and biogeographic history of the gartersnakes, watersnakes, and allies (Natricidae: Thamnophiini). *Molecular Phylogenetics and Evolution*, 186, 107844. https://doi.org/10.1016/j.ympev.2023.107844 580
 581
 582
 583
- Oaks, J. R. (2019). Full Bayesian Comparative Phylogeography from Genomic Data (L. Kubatko, Ed.). *Systematic Biology*, 68(3), 371–395. https://doi.org/10.1093/sysbio/syy063 584
 585
 586
- Oaks, J. R., Wood, P. L., Siler, C. D., & Brown, R. M. (2022). Generalizing Bayesian phylogenetics to infer shared evolutionary events. *Proceedings of the National Academy of Sciences*, 119(29), e2121036119. https://doi.org/10.1073/pnas.2121036119 587
 588
 589

- Portik, D. M., Streicher, J. W., & Wiens, J. J. (2023). Frog phylogeny: A time-calibrated, 590
species-level tree based on hundreds of loci and 5,242 species. *Molecular Phylogenetics and Evolution*, 591
188, 107907. <https://doi.org/10.1016/j.ympev.2023.107907> 592
- Pramuk, J. B., Robertson, T., Sites, J. W., & Noonan, B. P. (2007). Around the world 593
in 10 million years: Biogeography of the nearly cosmopolitan true toads (Anura: 594
Bufonidae). *Global Ecology and Biogeography*, 0(0), 070817112457001–???. <https://doi.org/10.1111/j.1466-8238.2007.00348.x> 595
- Pritchard, J. K., Stephens, M., & Donnelly, P. (2000). Inference of Population Structure 596
Using Multilocus Genotype Data. *Genetics*, 155(2), 945–959. <https://doi.org/10.1093/genetics/155.2.945> 597
- Pyron, R. A., & Wiens, J. J. (2011). A large-scale phylogeny of Amphibia including 598
over 2800 species, and a revised classification of extant frogs, salamanders, and 599
caecilians. *Molecular Phylogenetics and Evolution*, 61(2), 543–583. <https://doi.org/10.1016/j.ympev.2011.06.012> 600
- Reich, D., Thangaraj, K., Patterson, N., Price, A. L., & Singh, L. (2009). Reconstructing 601
Indian population history. *Nature*, 461(7263), 489–494. <https://doi.org/10.1038/nature08365> 602
- Rieseberg, L. H., Whitton, J., & Gardner, K. (1999). Hybrid zones and the genetic architecture 603
of a barrier to gene flow between two sunflower species. *Genetics*, 152(2), 604
713–727. 605
- Rochette, N. C., Rivera-Colón, A. G., & Catchen, J. M. (2019). Stacks 2: Analytical 606
methods for paired-end sequencing improve RADseq-based population genomics. 607
- Molecular Ecology*, 28(21), 4737–4754. <https://doi.org/10.1111/mec.15253> 608
- Wang, L.-G., Lam, T. T.-Y., Xu, S., Dai, Z., Zhou, L., Feng, T., Guo, P., Dunn, C. W., 609
Jones, B. R., Bradley, T., Zhu, H., Guan, Y., Jiang, Y., & Yu, G. (2020). Treeio: 610
An R Package for Phylogenetic Tree Input and Output with Richly Annotated 611
and Associated Data. *Molecular Biology and Evolution*, 37(2), 599–603. <https://doi.org/10.1093/molbev/msz240> 612
- 613
- 614
- 615
- 616
- 617

Weatherby, C. A. (1982). INTROGRESSION BETWEEN THE AMERICAN TOAD, BUFO AMERICANUS, AND THE SOUTHERN TOAD, B. TERRESTRIS, IN ALABAMA.	618
Wickam, H. (2016). Ggplot2: Elegant graphics for data analysis. <i>Springer-Verlag. Accessed March, 16, 2021.</i>	621
Yu, G., Smith, D. K., Zhu, H., Guan, Y., & Lam, T. T.-Y. (2017). Ggtree: An r package for visualization and annotation of phylogenetic trees with their covariates and other associated data. <i>Methods in Ecology and Evolution, 8</i> (1), 28–36. https://doi.org/10.1111/2041-210X.12628	623
	624
	625
	626

1.5 Figures

627

Sampling Distribution

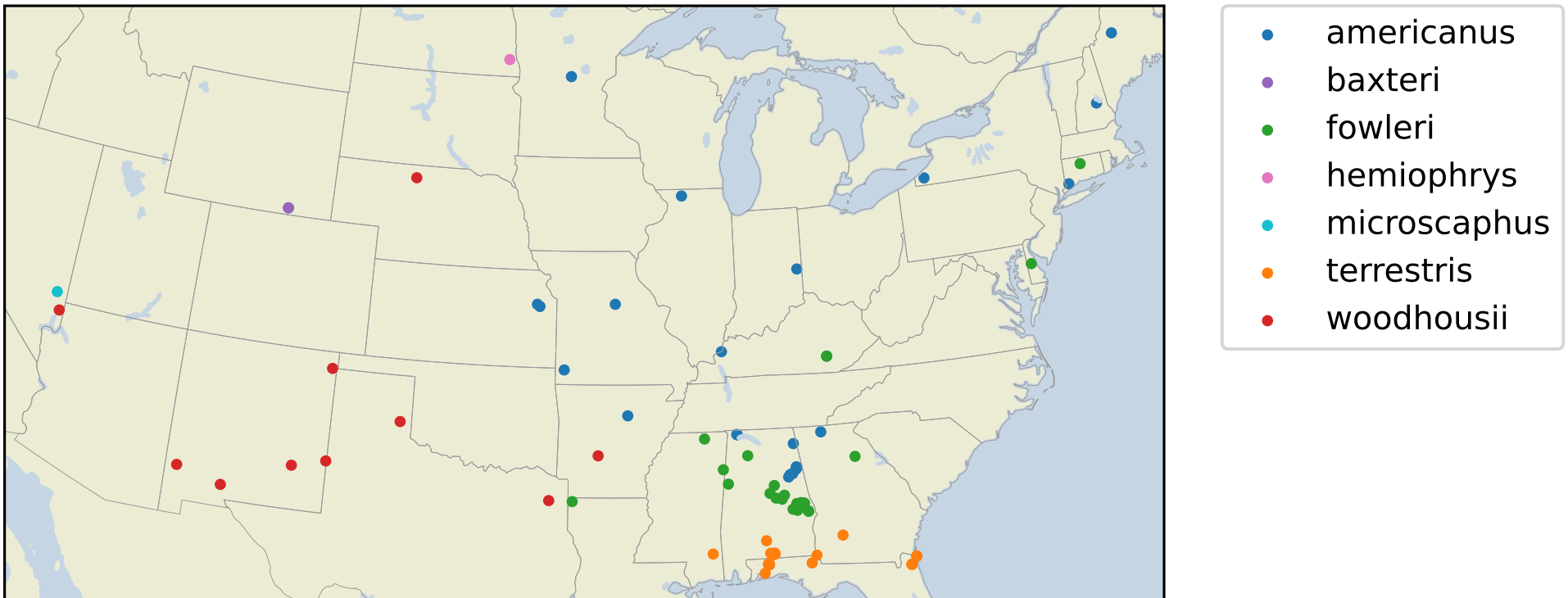


Figure 1.1. Distribution of *americanus* group samples

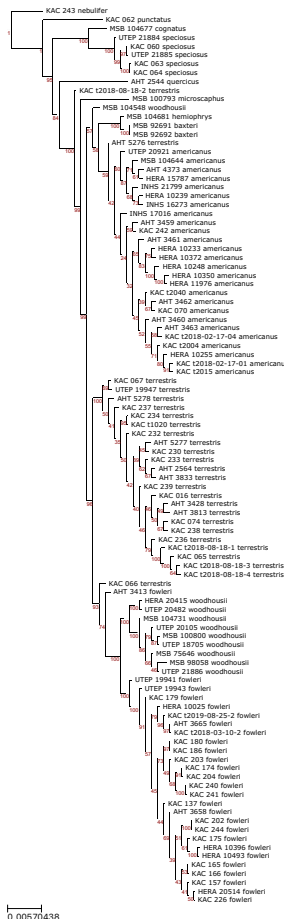


Figure 1.2. Maximum Likelihood Phylogeny Plotted using ETE 3.1.2 (Huerta-Cepas et al., 2016).

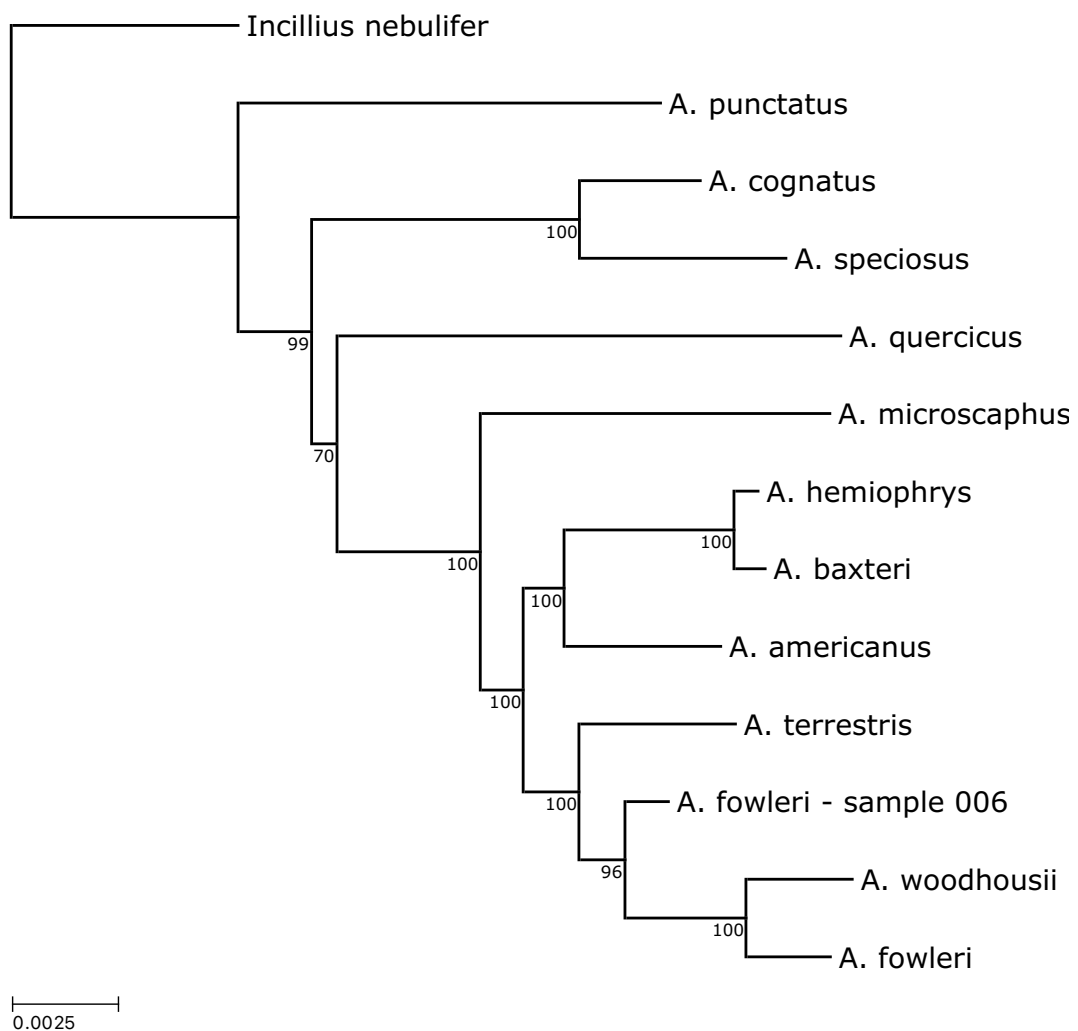


Figure 1.3. Maximum Likelihood Phylogeny with species clades collapsed. The lengths of tip branches are equal to the mean height of all collapsed tips from the base the collapsed clade. Plotted using ETE 3.1.2 (Huerta-Cepas et al., 2016).

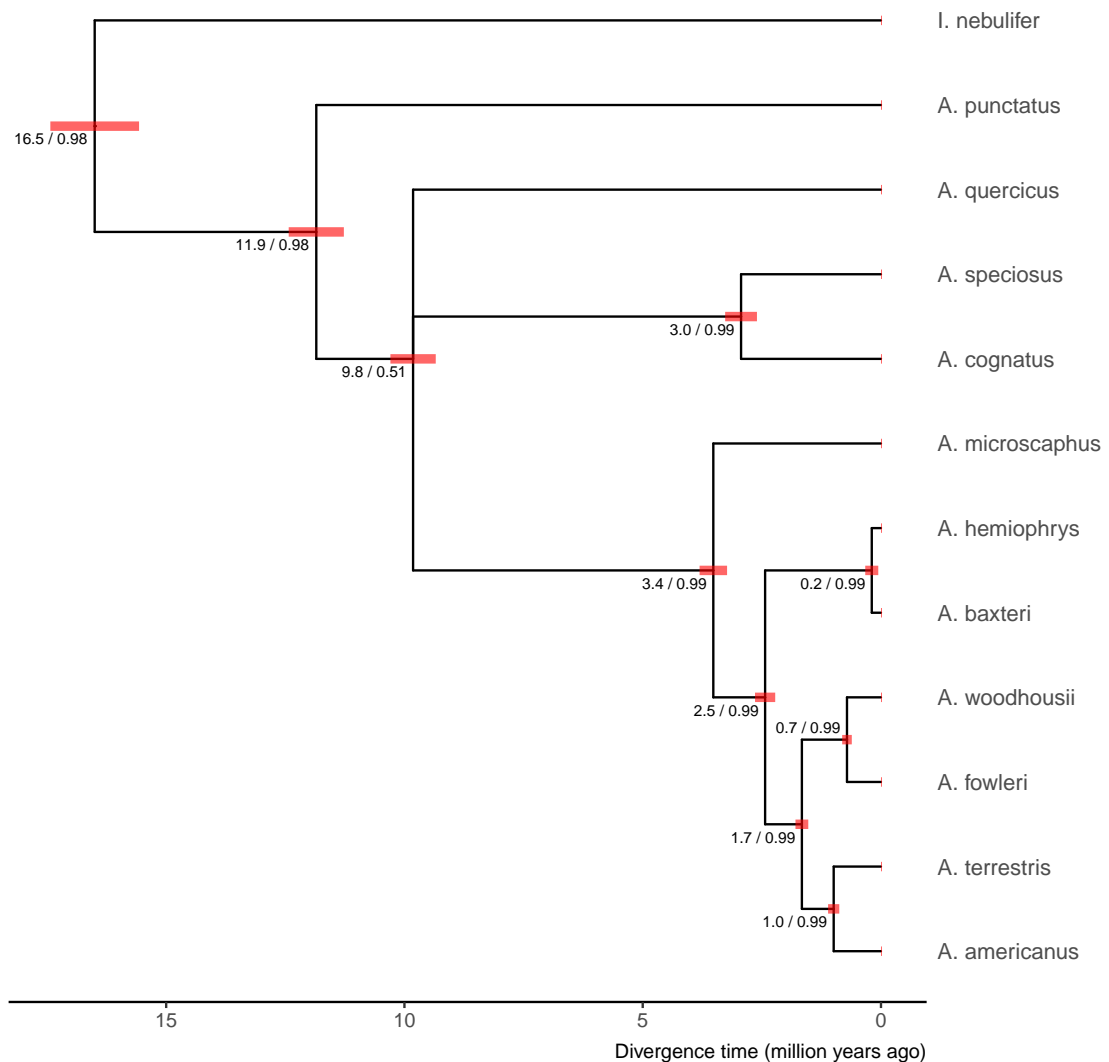


Figure 1.4. The maximum a posteriori tree inferred under a multispecies coalescent model by *phycoeval*. Branch lengths are rescaled from expected substitutions per site to millions of years using secondary time calibrations (*Materials and Methods*). Numbers displayed at each node are the mean posterior node age followed by the approximate posterior probability of the node rounded down to the nearest hundredth. Red bars show the 95% HPDI for the scaled node age at each node. Created using ggplot2 (Wickam, 2016), ggtree (Yu et al., 2017), and treeio (Wang et al., 2020)

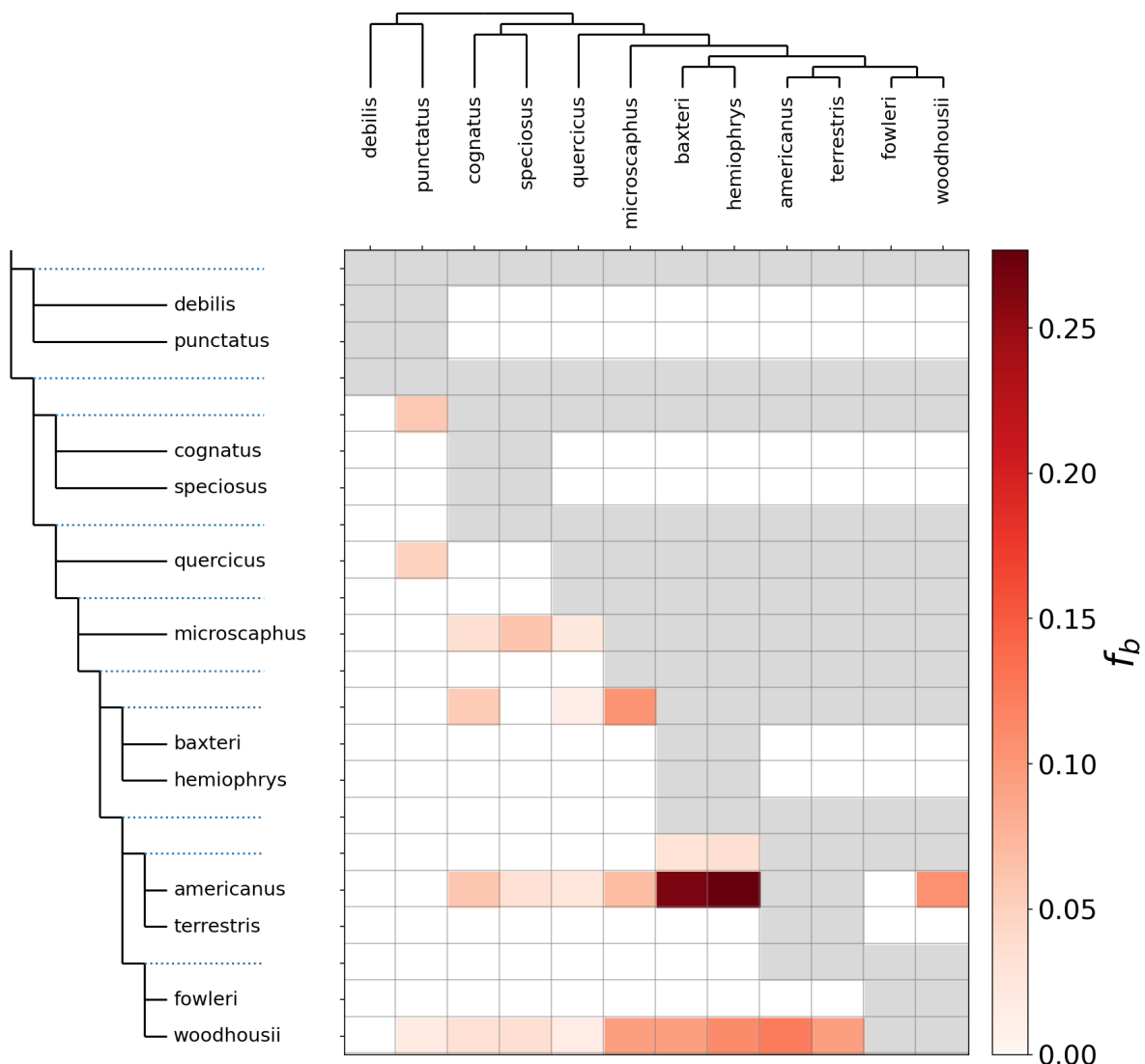


Figure 1.5. Heatmap showing the value of the f -branch statistic computed for all pairs possible pairs of *Anaxyrus* species. The f -branch statistic indicates the proportion of excess allele sharing between a species on the x-axis and branch on the y-axis (relative to its sister branch). Excess allele sharing between species identifies possible gene flow between them. Grey boxes indicate that the given tips cannot be tested by Dsuite for the given tree topology.

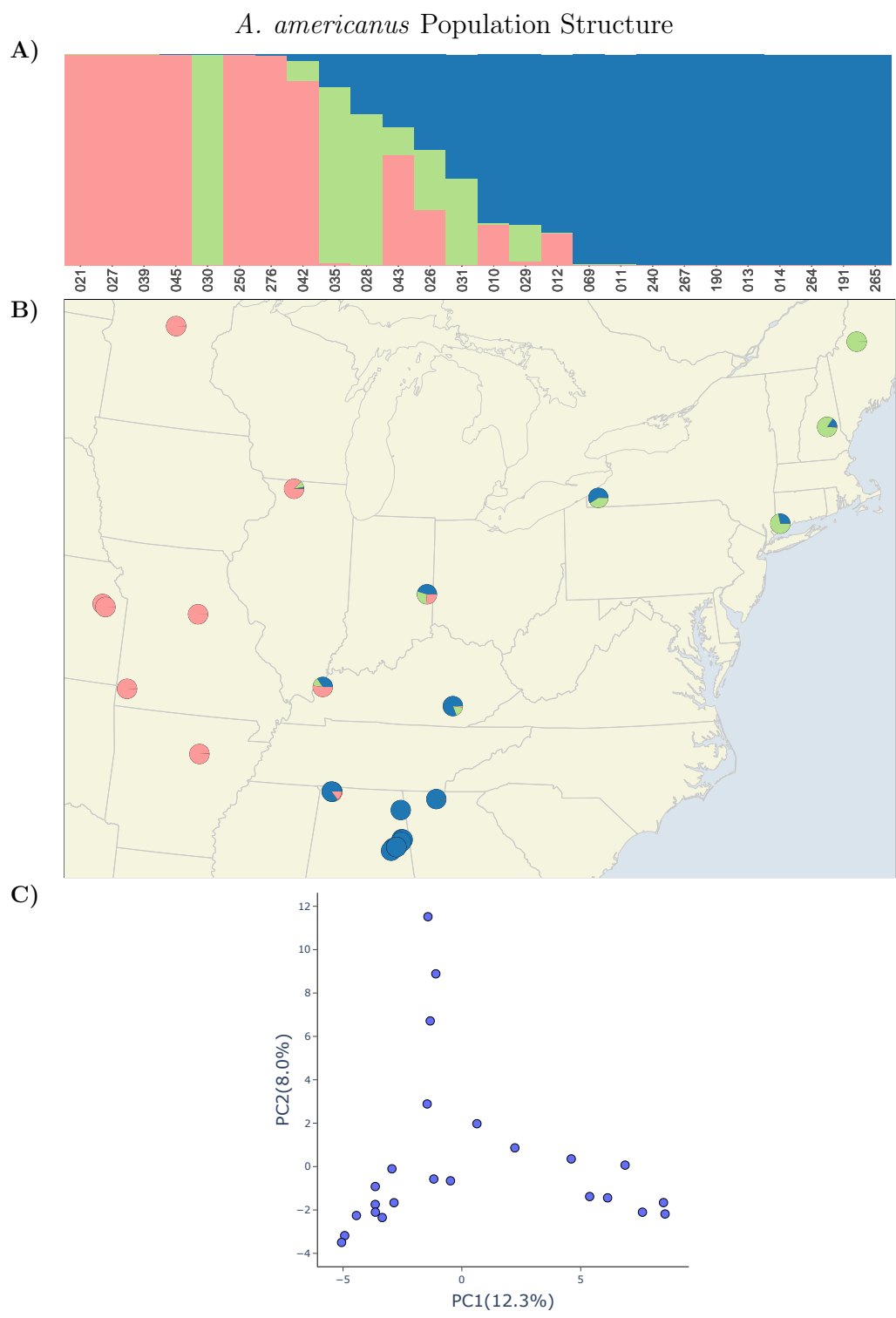


Figure 1.6. Population structure of *A. americanus* with PCA and map

A. fowleri Population Structure

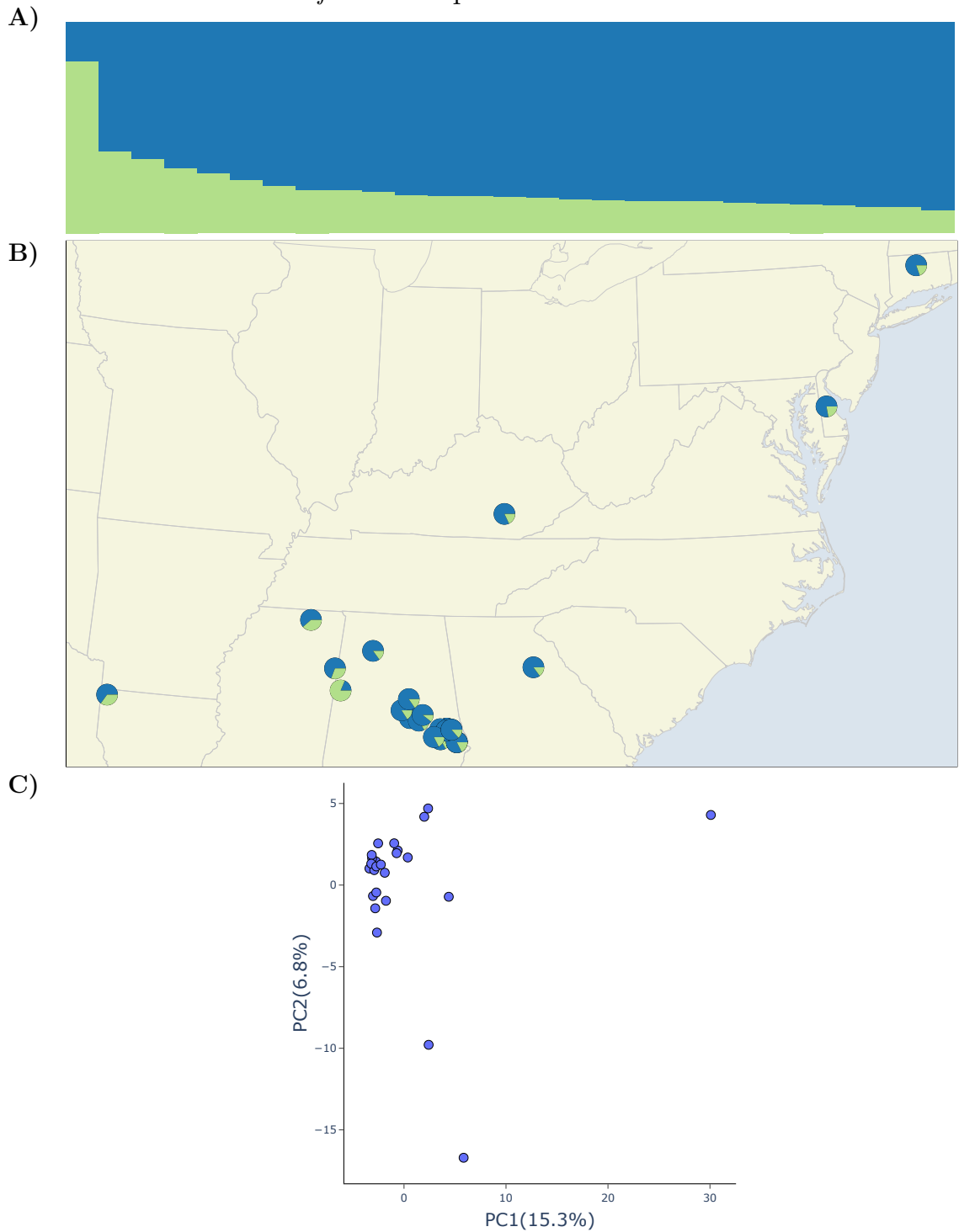


Figure 1.7. Population structure of *A. fowleri* with PCA and map

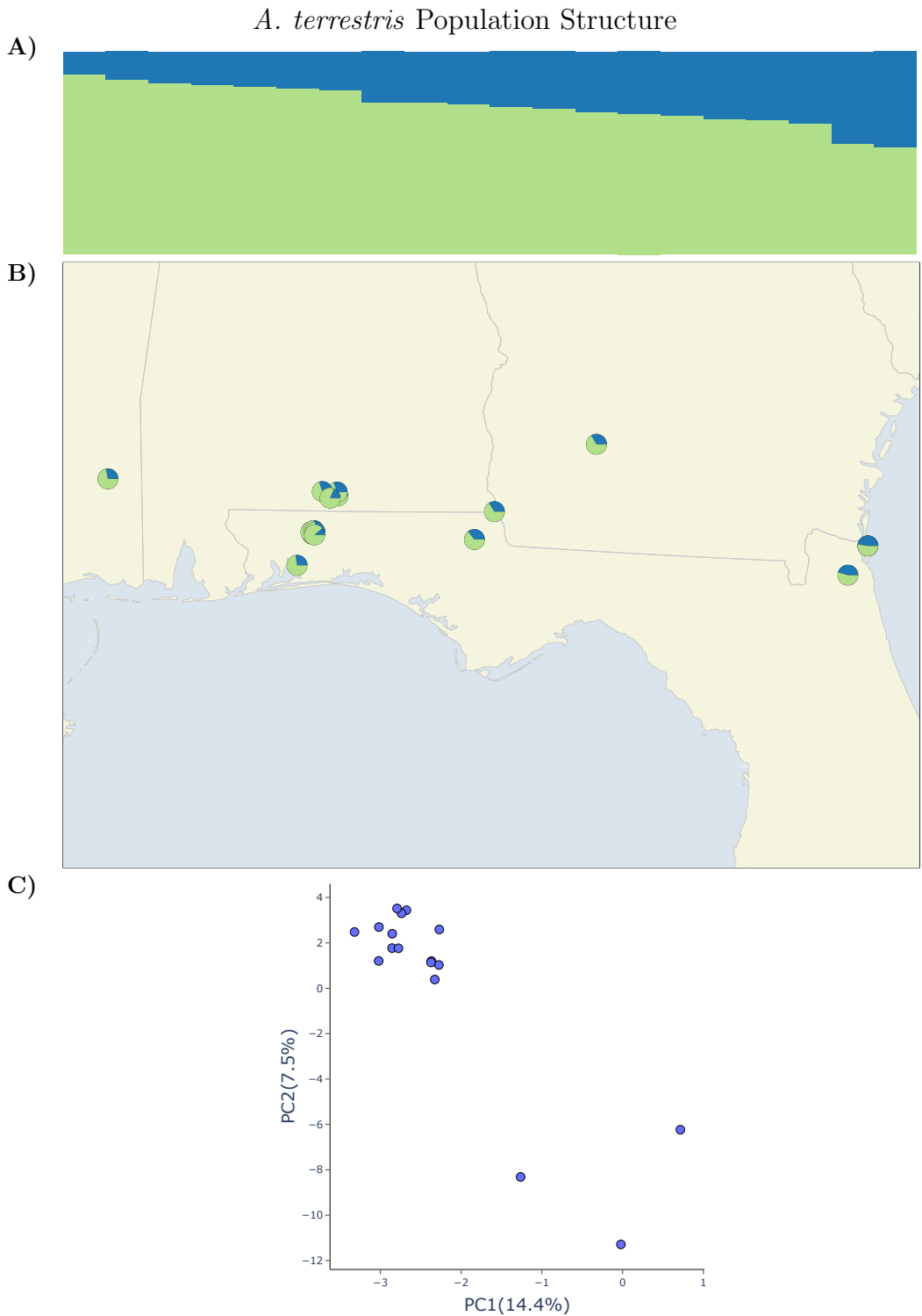


Figure 1.8. Population structure of *A. terrestoris* with PCA and map

A. woodhousii Population Structure

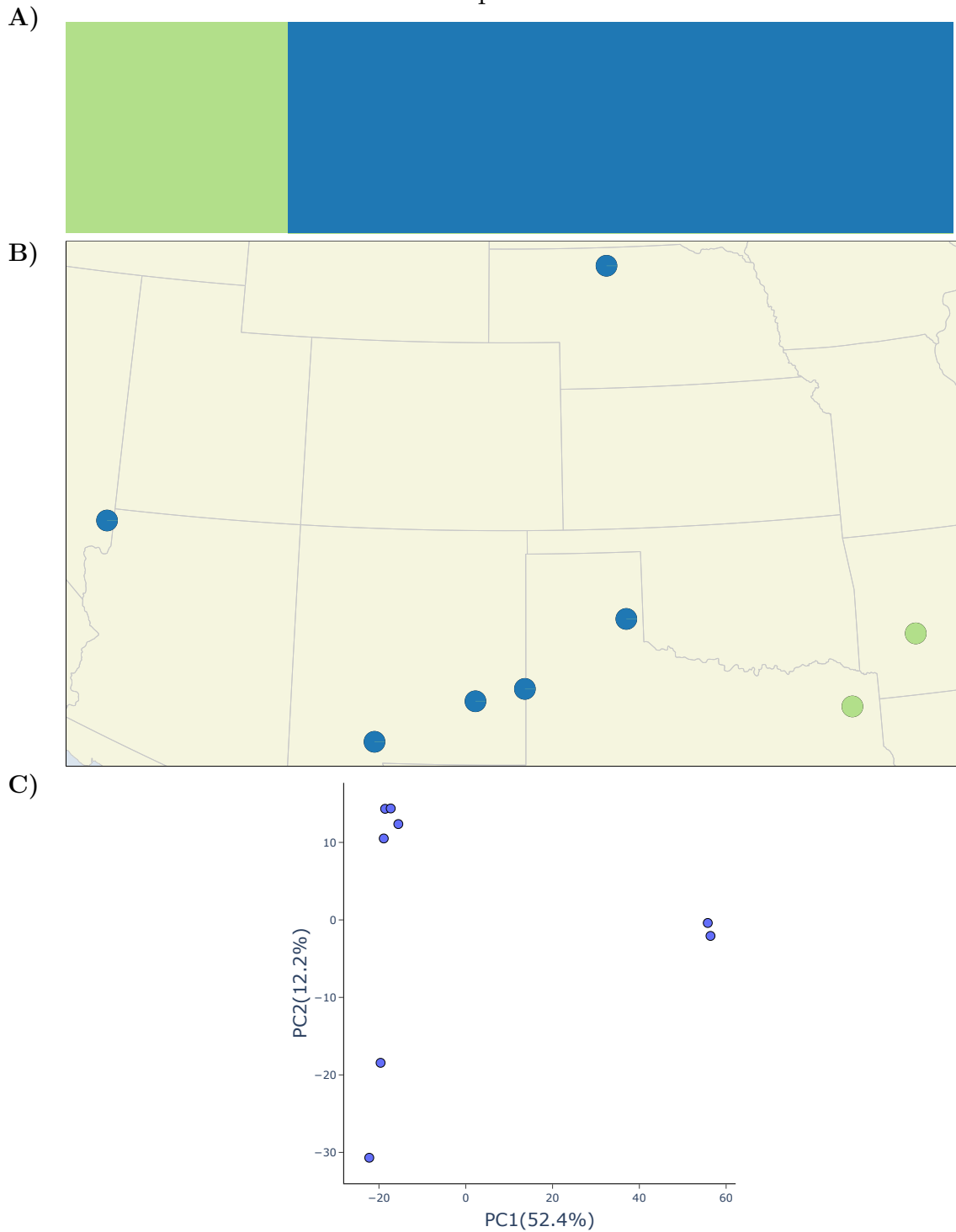


Figure 1.9. Population structure of *A. woodhousii* with PCA and map

A. fowleri + A. woodhousii Population Structure

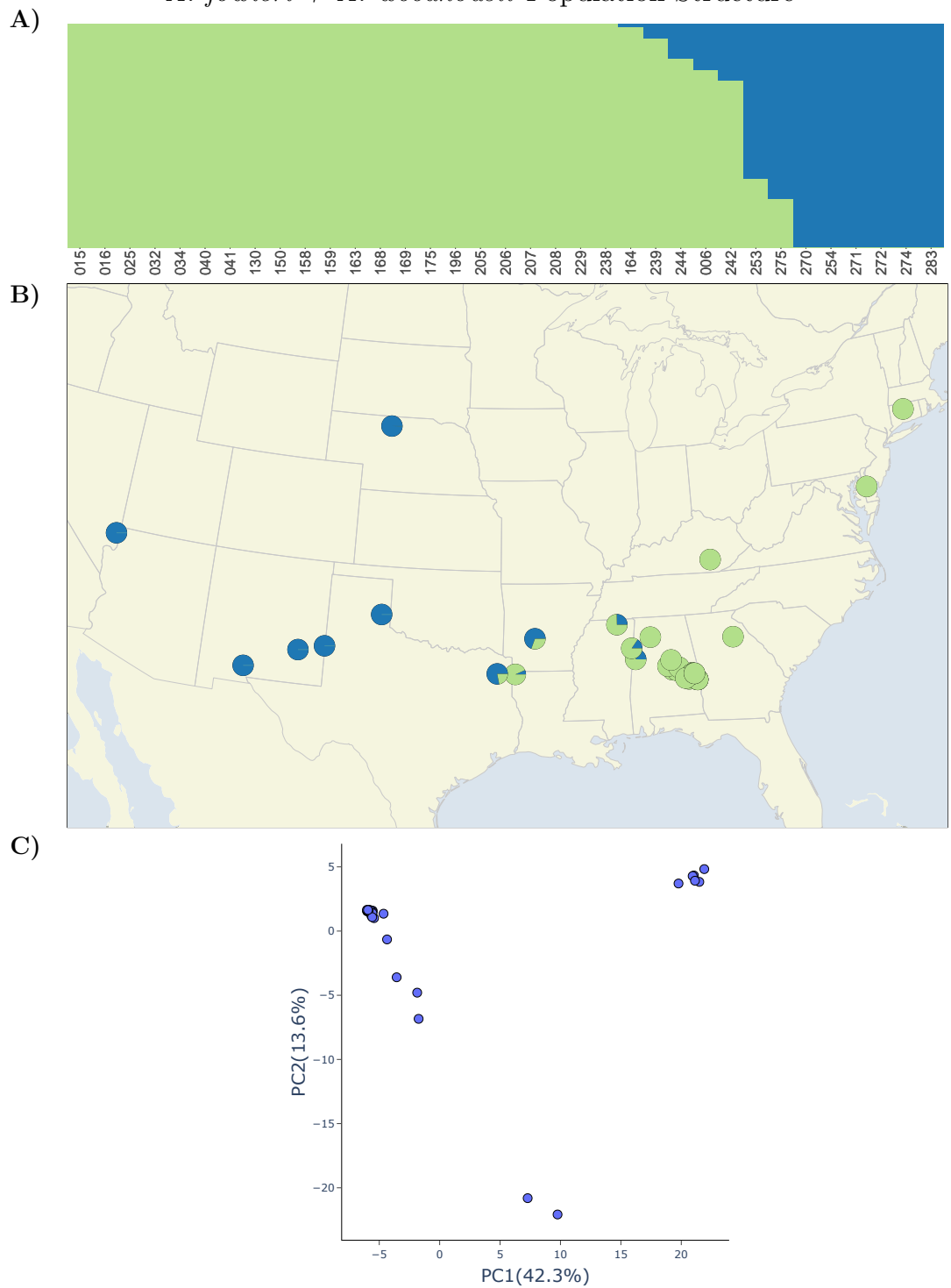


Figure 1.10. Population structure of *A. fowleri* with PCA and map

1.6 Tables

628

Table 1.1. Samples used in this study

ID	Sample ID	Species	Latitude	Longitude	Passed Filtering	Phycoeval	Structure
003	AHT 2544	<i>quercicus</i>	30.99523	-86.23332	X	X	
004	AHT 2564	<i>terrestris</i>	31.55752	-84.04267	X	X	X
006	AHT 3413	<i>fowleri</i>	33.36940	-88.12941	X		X
009	AHT 3428	<i>terrestris</i>	31.12679	-86.54755	X		X
010	AHT 3459	<i>americanus</i>	34.88028	-87.71849	X		X
011	AHT 3460	<i>americanus</i>	33.78013	-85.58421	X		X
012	AHT 3461	<i>americanus</i>	34.88779	-87.74103	X		X
68	013	AHT 3462	<i>americanus</i>	33.77001	-85.55434	X	X
	014	AHT 3463	<i>americanus</i>	33.71125	-85.59762	X	X
	015	AHT 3658	<i>fowleri</i>	32.85842	-86.39697	X	X
	016	AHT 3665	<i>fowleri</i>	32.81220	-86.17698	X	X
	017	AHT 3813	<i>terrestris</i>	31.13854	-86.53906	X	
	018	AHT 3833	<i>terrestris</i>	31.00422	-85.03427	X	X
	021	AHT 4373	<i>americanus</i>	38.94913	-95.39818	X	X
	022	AHT 5276	<i>terrestris</i>	31.55613	-86.82514		
	023	AHT 5277	<i>terrestris</i>	31.15830	-86.55430	X	X

Continued on next page

Table 1.1 – continued from previous page

ID	Sample ID	Species	Latitude	Longitude	Passed Filtering	Phycoeval	Structure
024	AHT 5278	<i>terrestris</i>	31.16105	-86.69868	X		X
025	HERA 10025	<i>fowleri</i>	37.11151	-84.11812	X	X	X
026	HERA 10233	<i>americanus</i>	39.86453	-85.01037	X	X	X
027	HERA 10239	<i>americanus</i>	38.99151	-92.31078	X		X
028	HERA 10248	<i>americanus</i>	41.27319	-73.38974	X		X
029	HERA 10255	<i>americanus</i>	37.11151	-84.11812	X		X
030	HERA 10350	<i>americanus</i>	45.51396	-69.95928	X	X	X
031	HERA 10372	<i>americanus</i>	42.22795	-79.36759	X		X
032	HERA 10396	<i>fowleri</i>	41.80663	-72.73281	X	X	X
033	HERA 10484	<i>marina</i>	25.61296	-80.56606			
034	HERA 10493	<i>fowleri</i>	39.08588	-75.56844	X	X	X
035	HERA 11976	<i>americanus</i>	43.51819	-71.42336	X		X
036	HERA 13722	<i>fowleri</i>	36.55514	-89.18929			
037	HERA 14196	<i>retiformis</i>	33.34906	-112.49010			
038	HERA 14926	<i>microscaphus</i>	33.73033	-113.98078			
039	HERA 15787	<i>americanus</i>	38.88546	-95.29399	X	X	X

Continued on next page

Table 1.1 – continued from previous page

ID	Sample ID	Species	Latitude	Longitude	Passed Filtering	Phycoeval	Structure
040	HERA 20415	<i>woodhousii</i>	34.31743	-92.94602	X	X	X
041	HERA 20514	<i>fowleri</i>	33.95140	-83.36715	X		X
042	INHS 16273	<i>americanus</i>	42.30245	-89.55950	X		X
043	INHS 17016	<i>americanus</i>	37.46121	-88.18728	X		X
044	INHS 19127	<i>fowleri</i>	41.58247	-88.07273			
045	INHS 21799	<i>americanus</i>	46.01258	-94.26710	X		X
046	KAC 016	<i>terrestris</i>	30.54819	-86.93067	X		X
061	KAC 053	<i>fowleri</i>	32.78044	-86.73877			
062	KAC 060	<i>speciosus</i>	27.69185	-99.71955	X		
063	KAC 062	<i>punctatus</i>	29.43603	-103.50564	X		
064	KAC 063	<i>speciosus</i>	29.29522	-103.92916	X		
065	KAC 064	<i>speciosus</i>	29.29522	-103.92916	X		
066	KAC 065	<i>terrestris</i>	30.43282	-81.64088	X		
067	KAC 066	<i>terrestris</i>	30.43282	-81.64088			
068	KAC 067	<i>terrestris</i>	30.43282	-81.64088			
069	KAC 070	<i>americanus</i>	34.79963	-84.57678	X		X

Continued on next page

Table 1.1 – continued from previous page

ID	Sample ID	Species	Latitude	Longitude	Passed Filtering	Phycoeval	Structure
071	KAC 074	<i>terrestris</i>	30.77430	-85.22690	X		X
130	KAC 137	<i>fowleri</i>	33.01461	-86.60953	X		X
150	KAC 157	<i>fowleri</i>	32.43769	-85.63620	X		X
158	KAC 165	<i>fowleri</i>	32.66356	-85.48498	X		X
159	KAC 166	<i>fowleri</i>	32.66356	-85.48498	X		X
163	KAC 174	<i>fowleri</i>	32.62938	-85.63828	X		X
164	KAC 175	<i>fowleri</i>	32.64849	-85.64711	X		X
167	KAC 178	<i>fowleri</i>	32.38644	-85.23561			
168	KAC 179	<i>fowleri</i>	32.38644	-85.23561	X		X
169	KAC 180	<i>fowleri</i>	32.38644	-85.23561	X		X
175	KAC 186	<i>fowleri</i>	32.38579	-85.23565	X		X
190	KAC t2018-02-17-01	<i>americanus</i>	33.55274	-85.82913	X		X
191	KAC t2018-02-17-04	<i>americanus</i>	33.48548	-85.88857	X		X
196	KAC t2018-03-10-2	<i>fowleri</i>	32.93116	-86.08465	X		X
200	KAC t2018-08-18-1	<i>terrestris</i>	30.66902	-81.44013	X		X
201	KAC t2018-08-18-2	<i>terrestris</i>	30.66902	-81.44013			

Continued on next page

Table 1.1 – continued from previous page

ID	Sample ID	Species	Latitude	Longitude	Passed Filtering	Phycoeval	Structure
202	KAC t2018-08-18-3	<i>terrestris</i>	30.43282	-81.64088	X	X	X
203	KAC t2018-08-18-4	<i>terrestris</i>	30.66902	-81.44013	X		X
205	KAC t2019-08-25-2	<i>fowleri</i>	34.21852	-87.36662	X		X
206	KAC 202	<i>fowleri</i>	33.25104	-86.43850	X		X
207	KAC 203	<i>fowleri</i>	32.62294	-85.49660	X		X
208	KAC 204	<i>fowleri</i>	32.62294	-85.49660	X		X
229	KAC 226	<i>fowleri</i>	32.48119	-85.79838	X		X
230	KAC 230	<i>terrestris</i>	30.80933	-86.77686	X		X
231	KAC 232	<i>terrestris</i>	30.80922	-86.78994	X		X
231	KAC 232	<i>terrestris</i>	30.80922	-86.78994	X		X
232	KAC 233	<i>terrestris</i>	30.80922	-86.78994	X		X
233	KAC 234	<i>terrestris</i>	30.80922	-86.78994	X		X
234	KAC 236	<i>terrestris</i>	30.82632	-86.80258	X		X
235	KAC 237	<i>terrestris</i>	30.83733	-86.77630	X		X
236	KAC 238	<i>terrestris</i>	30.82433	-86.76284	X		X
237	KAC 239	<i>terrestris</i>	30.80162	-86.76659	X		X

Continued on next page

Table 1.1 – continued from previous page

ID	Sample ID	Species	Latitude	Longitude	Passed Filtering	Phycoeval	Structure
238	KAC 240	<i>fowleri</i>	32.64328	-85.37114	X		X
239	KAC 241	<i>fowleri</i>	32.64328	-85.37114	X		X
240	KAC 242	<i>americanus</i>	34.50446	-85.63768	X		X
241	KAC 243	<i>nebulifer</i>	30.39140	-90.62049	X	X	
242	KAC 244	<i>fowleri</i>	32.89261	-93.88756	X		X
243	MSB 100793	<i>microscaphus</i>	37.27154	-114.46478	X	X	
244	MSB 100800	<i>woodhousii</i>	36.73612	-114.21972	X	X	X
245	MSB 100913	<i>microscaphus</i>	33.28038	-108.08868		X	
246	MSB 104548	<i>woodhousii</i>	36.49094	-103.20838			
247	MSB 104570	<i>fowleri</i>	34.00087	-95.38229			
248	MSB 104571	<i>americanus</i>	34.00917	-95.38058			
249	MSB 104608	<i>americanus</i>	34.00367	-94.82670			
250	MSB 104644	<i>americanus</i>	36.95124	-94.27782	X		X
251	MSB 104677	<i>cognatus</i>	46.39834	-97.20927	X	X	
252	MSB 104681	<i>hemiophrys</i>	46.47076	-97.04604	X		X
253	MSB 104731	<i>woodhousii</i>	42.61091	-100.65607	X	X	X

Continued on next page

Table 1.1 – continued from previous page

ID	Sample ID	Species	Latitude	Longitude	Passed Filtering	Phycoeval	Structure
254	MSB 75646	<i>woodhousii</i>	33.36365	-104.34282	X	X	X
255	MSB 92689	<i>baxteri</i>	41.21182	-105.82558			
256	MSB 92691	<i>baxteri</i>	41.21182	-105.82558	X	X	
257	MSB 92692	<i>baxteri</i>	41.21182	-105.82558	X	X	
258	MSB 96528	<i>debilis</i>	32.58239	-107.46348			
259	MSB 98058	<i>woodhousii</i>	32.83360	-108.60900			
260	MSB 98065	<i>cognatus</i>	32.63240	-108.73800		X	
261	KAC t1020	<i>terrestris</i>	31.10783	-86.62247	X		X
264	KAC t2004	<i>americanus</i>	33.58295	-85.73524	X		X
265	KAC t2015	<i>americanus</i>	33.58435	-85.74064	X		X
267	KAC t2040	<i>americanus</i>	33.58295	-85.73539	X		X
269	KAC t3040	<i>fowleri</i>	32.38644	-85.23561			
270	UTEP 18705	<i>woodhousii</i>	32.45198	-106.88317	X	X	X
271	UTEP 19941	<i>fowleri</i>	34.79137	-88.95715	X	X	X
272	UTEP 19943	<i>fowleri</i>	33.81998	-88.29533	X		X
273	UTEP 19947	<i>terrestris</i>	31.22432	-88.77548	X	X	X

Continued on next page

Table 1.1 – continued from previous page

ID	Sample ID	Species	Latitude	Longitude	Passed Filtering	Phycoeval	Structure
274	UTEP 20105	<i>woodhousii</i>	33.62853	-103.08198	X		X
275	UTEP 20482	<i>woodhousii</i>	32.90708	-94.74945	X		X
276	UTEP 20921	<i>americanus</i>	35.55405	-91.83443	X		X
277	UTEP 21284	<i>debilis</i>	31.25968	-105.33402		X	
278	UTEP 21286	<i>speciosus</i>	31.70140	-105.47958			
279	UTEP 21724	<i>speciosus</i>	31.26087	-104.60168			
280	UTEP 21881	<i>cognatus</i>	35.53600	-100.44035		X	
281	UTEP 21884	<i>speciosus</i>	32.75472	-101.43208	X		
282	UTEP 21885	<i>speciosus</i>	32.20195	-100.34345	X		X
283	UTEP 21886	<i>woodhousii</i>	35.07800	-100.43392	X		X